CO_2 adsorption/desorption in FAU zeolite nanocrystals: *in situ* synchrotron X-ray powder diffraction and *in situ* FTIR spectroscopic study

Michelangelo Polisi,[1] Julien Grand,[2] Rossella Arletti,[3,*] Nicolas Barrier,[4] Sarah Komaty,[2] Moussa Zaarour,[2] Svetlana Mintova,[2,*] Giovanna Vezzalini[1]

[1]Dipartimento di Scienze Chimiche e Geologiche, Università di Modena e Reggio Emilia, Italy
[2]Normandie Univ, ENSICAEN, UNICAEN, CNRS, Laboratoire Catalyse et Spectrochimie, Caen, France.
[3]Dipartimento di Scienze della Terra, Università di Torino, Italy
[4]Laboratoire de Cristallographie et Sciences des Matériaux (CRISMAT), Normandie Université, ENSICAEN, CNRS, Caen, France

Abstract: The host-guest and guest-guest interactions governing the CO_2 adsorption/desorption in two nanosized zeolite samples with FAU framework type and different Si/Al ratios (Na-X Si/Al=1.24 and Na-Y Si/Al=2.54) and cations distribution were investigated by *in situ* synchrotron high resolution X-ray powder diffraction (XRPD) and *in situ* FTIR spectroscopy. The two complementary techniques allow probing the CO_2 adsorption/desorption in the FAU zeolites at different levels, i.e. average structure by XRPD *vs* local structure by IR. The presence of physisorbed CO_2 molecules in both zeolites was detected by XRPD, while only a high amount of chemisorbed CO_2 in the Na-X zeolite was found. The presence of unshielded Na cations and H_2O molecules in the supercage of the Na-X sample induces the formation of stable bidentate bicarbonate groups. The evacuating of CO_2 loaded samples resulted in an efficient removal of physisorbed CO_2 from both nanosized zeolites, on the contrary high temperature is required to remove the chemisorbed species from the nanosized Na-X zeolite. Understanding the CO_2 sorption behavior and capacity of nanosized zeolites is of great importance in broadening their use in environmental, clinical and biomedical applications.

1. Introduction

The continuous increase of carbon dioxide in the atmosphere is one of the main causes of climate change[1]. As long as the global energetic is satisfied by the combustion of carbon-based fossil fuels, serious environmental problems, such as reducing the CO_2 emission, must be faced with efficient solutions.

Different technologies have been examined in the last years in order to capture and separate CO_2 from flue gases. CO_2 capture in solid systems provides a way to permanently store, easily transport, and possibly extract carbon dioxide, skipping the technical and environmental difficulties involved in large scale direct stocking into the Earth's depths.

Several studies have explored methods of separation using materials that can operate via weak physisorption interactions or strong chemisorption processes, such as activated carbon materials, polymers, calcium oxides, microporous and mesoporous materials[2,3]. Reactions, characterized by CO_2 trapping via open structure solid state systems (for instance microporous materials such as zeolites and MOF), allow to tune CO_2-equilibrium in a given environment, and represent an efficient way of low-energy-storage/release of carbon dioxide.

Zeolites are appropriate candidates for selective adsorption and separation of carbon dioxide[4], not only due to their high adsorption capacity and their particularly low price[3,5], but also because of their properties (i.e. crystal size, pore architecture, chemical composition, nature of extra-framework cations).

Particular attention has been paid to faujasite type zeolites (FAU framework type[6]), which are considered as possible candidates for CO_2 separation process. The adsorption performances of FAU type zeolites, either zeolite X or Y, were investigated with different methods. Lee *et al.*[7] and Lu *et al.*[8] found that zeolite 13X possesses higher adsorption capacity for CO_2, and a more favorable adsorption, with respect to activated carbon composites. Siriwardane et al.[9] report that 13X zeolite shows preferential adsorption for CO_2 from a gas mixture representing coal combustion compared to other commercial zeolites (4A, 5A, APG-II and WE-G 592). Also computational studies[10,11] indicate zeolites X and Y as the most promising adsorbents for CO_2 storage. Recently, experimental structural studies have been carried out to investigate the adsorption properties of zeolite Na-Y by both neutron[12] and synchrotron X-ray powder diffraction[13]. Both studies indicated that the cations and water molecules distribution in the pores of zeolites strongly affects the CO_2 adsorption/desorption dynamics.

In order to exploit the material functionalities and to design tailor-made materials, it is of paramount importance to unravel the mechanisms that underlie the CO_2 trapping phenomena by understanding the host–guest interactions. Moreover, the interest in nanosized zeolites strongly increased in the last few years owing to the potential variation of their properties as a function of the size[14]. The advantages of the use of nanosized zeolites lie in their unique properties such as tunable crystal size, chemical composition, larger external surface areas, reduced diffusion path lengths and more accessible active sites compared to micron-sized zeolite crystals. On the other hand, the size of zeolite plays a major role when it comes to biomedical applications. The modifications of zeolite

crystal size, from micron to nanoscale yielding biocompatible nanozeolites become of important research field. The target delivery of CO_2 by nanozeolites is considered as an essential moderator in human physiology, controlling blood circulation and pH[15,16,17].

In this work, the CO_2 adsorption/desorption mechanism in two nanosized zeolite samples with FAU framework type having different Si/Al ratios, cations, and particle size distribution is investigated. Combined *in situ* synchrotron high resolution X-ray powder diffraction (XRPD) and *in situ* FTIR spectroscopy experiments were carried out to unravel the host-guest and guest-guest interactions governing the CO_2 adsorption/desorption mechanism.

2. Experimental

2.1 Na-X and Na-Y zeolites synthesis

Materials

The following initial reagents were used for preparation of the precursor mixtures: Al powder (Al, 325 mesh, 99.5 %, Alfa Aesar); Aluminum hydroxide ($Al(OH)_3$, Sigma-Aldrich); Sodium aluminate (Al_2O_3 ~ 50-56 wt. %, Na_2O ~ 40-45 wt. %, Sigma-Aldrich); Sodium hydroxide (NaOH, Sigma-Aldrich, 97 %); Colloidal silica (SiO_2, Ludox-HS 30, 30 wt. % SiO_2, pH=9.8, Sigma ~~??~~Aldrich); Sodium silicate (SiO_2 ~ 26.5 wt. %; Na_2O, ~10 wt. %, Aldrich).The zeolite samples were prepared following a procedure recently published by our group~~.~~[18] .

Na-X. The nanosized zeolite Na-X was synthesized from a clear precursor suspension. The initial reactants were mixed to prepare two initial solutions denoted A and B according to the following procedure:

Solution A was prepared by dissolving 2.5 g of NaOH in 3 g dd H_2O followed by slow addition of 0.297 g alumina powder (325 mesh, 99.5 %); *Solution B was* prepared by mixing 10 g colloidal silica (Ludox-HS 30, 30 wt. % SiO_2, pH=9.8) with 1.1 g NaOH and 1 g dd H_2O. Solution A was added drop wise under vigorously stirring to the solution B (solution B was kept in ice during the mixing). The resulting clear suspension was aged 24 h at room temperature, and then the water content was adjusted to obtained a colloidal precursor suspension with the following composition: 10 SiO_2: 1.1 Al_2O_3: 9 Na_2O: 50 H_2O. The hydrothermal crystallization was conducted at 50 °C for 24 h. After crystallization, the suspensions were purified by high-speed centrifugation (20000 rpm, 100 min). The resulting solid was washed with doubly distilled water until pH 7.5 is reached. The nanosized crystals were freeze-dried to prevent their irreversible agglomeration.

Na-Y . The nanosized Na-Y zeolite was synthesized from a clear precursor suspension. The initial

Formattato: Nessun controllo righe isolate, Non regolare lo spazio tra testo asiatico e in alfabeto latino, Non regolare lo spazio tra testo asiatico e caratteri numerici

reactants were mixed to prepare two initial solutions denoted as A and B according to the following procedure: *Solution A was* prepared by dissolving 0.65 g of sodium aluminate in 3 g double distilled water (dd H_2O)*; Solution B was* prepared by mixing of 13 g colloidal silica (Ludox-HS 30, 30 wt. % SiO_2, pH=9.8) with 2.5 g NaOH and 0.98 g (dd) H_2O. Solution A was added drop wise under vigorously stirring to the solution B (solution B was kept in ice during the mixing). The resulting clear suspension was aged four days at room temperature. A colloidal precursor suspension with the following composition was obtained: 10 SiO_2: 0.7 Al_2O_3: 6.5 Na_2O: 122 H_2O. The hydrothermal crystallization was conducted at 100 °C for 2 h. The crystalline product was purified and dried as described for zeolite Na-X.

2.2 Characterization of Na-X and Na-Y zeolites

2.2.1 Dynamic Light Scattering analysis (DLS): The size of the zeolite nanoparticles was measured by a Malvern Zetasizer Nano instrument using a backscattering geometry (scattering angle of 173°, He−Ne laser with a 3 mW output power at a wavelength of 632.8 nm). The DLS analyses were performed on samples in water suspensions with a solid concentration of 1 wt. %.

2.2.2 Transmission Electron Microscopy (TEM) imaging: The crystal size, morphology and crystallinity of zeolites were determined by a transmission electron microscopy (TEM) using a Titan 80-300 operating at 300 kV.

2.2.3 Inductively Coupled Plasma (ICP) analysis: The chemical composition of the zeolites was determined by inductively coupled plasma optical emission spectroscopy using a Varian ICP-OES 720-ES; the chemical composition of nanosized zeolites are shown in Table 1.

2.2.4 N_2 adsorption analysis: The porosity of the samples was measured using a Micrometrics ASAP 2020 volumetric adsorption analyzer. Samples were degassed at 275 °C under vacuum overnight prior to the measurement. The external surface area and micropore volume were estimated by ~~t~~??-plot method using Silica-1000 (22.1 m^2 g^{-1} assumed) as a reference. The micropore and mesopore size distributions of solids were estimated by the Nonlocal Density Functional Theory (NLDFT) and Barret-Joyner-Halenda (BJH) on the desorption branch methods, respectively.

2.2.5 Thermogravimetric analysis: The moisture content and stability of samples were investigated using a SETSYS instrument (SETARAM) analyzer (heating rate of 5 °C min^{-1} under 40 $ml.min^{-1}$ flow of air).

Formattato: SpazioDopo: 0 pt

2.2.6 *In situ* FTIR study using CO_2 as a probe molecule: The adsorption of CO_2 on Na-X and Na-Y samples was investigated using FTIR spectroscopy. Powders were pressed (~10^7 Pa) into self-supported discs (2 cm^2 area, ~20 mg) and placed in an IR cell equipped with KBr windows. IR spectra were recorded using a Nicolet 6700 IR spectrometer with a MCT detector and an extended-KBr beam splitter was used. Spectra were recorded in the 400–5500 cm^{-1} range with a resolution of 4 cm^{-1} and 128 scans were collected for each spectrum. A movable quartz sample holder allowed placing the self-supported discs in the infrared beam, for recording spectra, and moving it into a furnace at the top of the cell for thermal treatment. The cell was connected to a high vacuum line with a reachable pressure of ~10^{-9} Bar. The samples were activated in a two-steps process: (i) 100 °C for 0.5 h to desorb most the physisorbed water, and (ii) 250 °C for 2 h, to remove any chemisorbed water. Both steps were performed under secondary vacuum (~$5 \cdot 10^{-9}$ Bar). Small CO_2 doses were introduced into the FTIR cell at room temperature and kept in equilibrium for 15 minutes. High vacuum desorption was then conducted at room temperature (*RT*) for 15 minutes, followed by desorption at 250 °C for 15 minutes.

2.2.7 *In situ* X-Ray Powder Diffraction (XRPD) study: Synchrotron XRPD experiments were performed on the high resolution beamline ID22 at ESRF (Grenoble - France) with a fixed wavelength of 0.3999 Å. The two samples Na-Y and Na-X were packed in 0.7 quartz capillaries and mounted on a support connected to a gas-rig. The samples were heated in-situ using a hot-air blower with a heating rate of 3 °C/min from room temperature (*RT*) to 250°C and evacuated nominally to 5 10^{-3} Torr by means of a turbo vacuum pump to favor water release. Once dehydrated, the samples were kept at *RT*. CO_2 was sent into the capillaries (maximum pressure of 1.85 and 1.5 bar for Na-Y and Na-X, respectively) and equilibrated for 15 minutes. Then the samples were pumped 10 minutes to test the CO_2 persistence in zeolite porosities.

Diffraction patterns were recorded at different times with a high-resolution multi-analyzer, composed of nine analyzer crystals, in the 2θ range 0–26° (data collection time: 37 minutes). For both samples data collections were performed as follows: (1) at *RT* (samples named Na-X-*RT*, Na-Y-*RT*); (2) at 250° C (samples named Na-X-*D-HT*, Na-Y-*D-HT*); (3) at *RT* after dehydration (samples named Na-X-*D-RT*, Na-Y-*D-RT*); (4) after CO_2 loading (samples named Na-X-*CO_2* , Na-Y-*CO_2*); (5) at *RT* after pumping (samples named Na-X-*AP*, Na-Y-*AP*).

2.2.8 Structural Refinements: All structure refinements of Na-X and Na-Y samples were performed with Rietveld method using GSAS package[19] with EXPGUI interface[20]. To locate the loaded CO_2 molecules in both zeolite samples, the starting stages of refinement were carried out in the space group (s.g.) *Fd-3,* using the framework coordinates published by Su and co-workers[21]. Sodium cations, water and CO_2 molecules were found by difference Fourier maps. After the localization of the extra-framework species, the refinement suggested a higher symmetry for the Na-Y zeolite. For this sample, the Fd-3m s.g. and the model of Olson and co-workers[22] were used for all refinements. Lattice parameters and refinement details are presented in Table S1, Observed and calculated pattern after Rietveld refinement are reported in Figure S1a-h. The Bragg peak profiles were modeled by a pseudo-Voigt function[23], and peak intensity cut-off was set to 0.01 of the peak maximum. The background curve was fitted by a Chebyshew polynomial with a variable number of coefficient from 15 to 30. The 2θ-zero shift, the overall scale factor and the unit cell parameters were refined accurately in each cycle. Soft constraints were imposed on the tetrahedral T-O lengths (1.63 Å), and on the C-O lengths of the CO_2 molecules (1.18 Å) and the tolerance value was set at 0.03. The isotropic thermal displacement parameters of the framework oxygen atoms were constrained to the same value. For samples Na-X-*RT* and Na-Y-*RT* also the thermal displacement parameters of the water molecules were refined constrained to the same value.

3. Results and Discussion

3.1 Zeolites characterization

TEM images show the high crystallinity of both samples. The Na-X and Na-Y zeolites present uniform and highly crystalline particles with average size of 20 nm and 150 nm, respectively (Figure 1a,b). The homogeneous zeolite nanocrystals exhibit a typical octahedral morphology with fully crystalline and well-developed faces, which become more pronounced in the case of Na-Y. The DLS curves for Na-X and Na-Y samples confirm the narrow, monomodal particle size distribution of the crystals (Figure 1c). The back-scattering of light produced from these samples was strong enough to be monitored as a function of the particle numbers. The cumulant analysis gives an average particle diameter, which is located between the minimum and maximum particle sizes present in the samples (Figure 1c**)**. The value of the polydispersity index for both measurements is 0.05, which shows that the samples contain particles with a very narrow particle size distribution. These DLS results are consistent with the TEM measurements (Figure 1a,b).

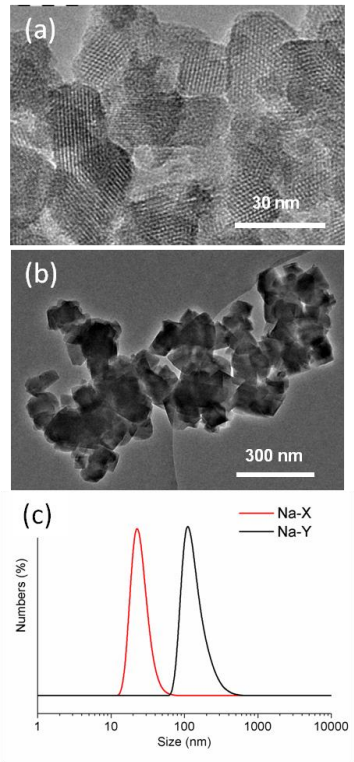

Figure 1. TEM images of as prepared (a) Na-X and (b) Na-Y samples, and (c) DLS curves of zeolite suspensions with a solid content of 1 wt. %.

The chemical composition of the samples determined by ICP analysis are presented in Table 1. The Si/Al ratios for nanosized Na-X and Na-Y samples are 1.24 and 2.54 wt. %, respectively.

Table 1. Chemical composition of nanosized Na-X and Na-Y zeolite samples determined by ICP.

Sample	Si (wt. %)	Al (wt. %)	Na (wt. %)	Si/Al
Na-X	19.5	15.8	14.5	1.24
Na-Y	43.1	17.0	15.4	2.54

The amount of water in both samples was determined by thermogravimetric analysis (TG). The TG/dTG results of the samples are shown in Figure 2. The dTG curve of Na-X zeolite shows two main mass losses at 100 °C and 146 °C corresponding to water adsorbed in the channels and on

the surface of the zeolite nanoparticles and differently bonded, contributing to 25 wt. % of its total mass loss. The Na-Y zeolite shows only one peak at 102 °C, contributing to 19 wt.% loss of its total mass.

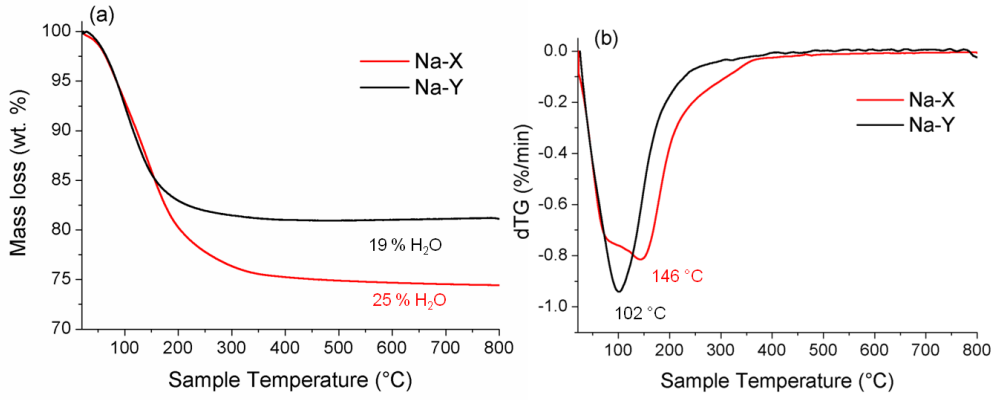

Figure 2. (a) Thermogravimetric (TG) and (b) differential thermogravimetric (dTG) curves of Na-X and Na-Y zeolite samples.

Considering the results from the TG and ICP analyses, the chemical formulas representing the nanosized Na-X and Na-Y zeolite samples are as follow:

$$\text{Na-X: } Na_{94.5}(Al_{87.6}Si_{104.4}O_{384}) \cdot 252\ H_2O \text{ (Si/Al = 1.19)}$$

$$\text{Na-Y: } Na_{59.5}(Al_{55.9}Si_{136.1}O_{384}) \cdot 167\ H_2O \text{ (Si/Al = 2.43)}$$

3.2 In situ XRPD characterization of nanosized zeolites

Structural features of hydrated nanosized zeolites

The *in situ* XRPD measurements at *RT* and the corresponding Rietveld refinement allowed to obtain a snapshot of the structure features of both samples before dehydration and CO_2 adsorption/desorption cycling. In particular, the position of the extra-framework species (cations and H_2O molecules), which plays an important role in the CO_2 sorption mechanism, was determined in both samples.

In the Na-X sample, four crystallographic independent Na sites were identified: Na2, Na2', Na3, Na6 (labelled after Olson[22~~19~~]) (Figure 3a). Na2 and Na2' sites are in the sodalite cages and correspond to site I and I' according to the conventional classification[24]. Na3 site is located at the

center of the hexagonal window between the sodalite cage and the supercage and corresponds to site II[24~~21~~]. Site Na6 is in the supercage near the site III'b[21~~18~~]. The total amount of sodium is 96.5 atoms p.u.c., which is in good agreement with the ICP analysis (94.5 atoms p.u.c.). Six crystallographic independent water sites were found, accounting for a total of 250 H_2O molecules, which is in good agreement with 252 molecules p.u.c. determined by TG analysis. Five water molecules are located in the supercage, coordinated to the Na6 cations or to the framework oxygen atoms, and one in the sodalite cage coordinated to Na2' cations (for structure details see Tables S2 and S3).

The same Na sites were found in the Na-Y sample, with the exclusion of site Na6 located in the supercage (Figure 3). The sodium total amount is 55.4 atoms p.u.c., which is in good agreement with the ICP results (59.5 Na p.u.c.). Five positions, accounting for 235 water molecules p.u.c., were located in the supercage: two of them coordinated to framework oxygen atoms and one coordinated to the Na4 cations (Tables S2 and S3). While the water content calculated by the Rietveld refinement for the Na-X is similar to that determined by the TG analysis, in the case of Na-Y, a higher amount of water was obtained by the refinement. The difference could be related to the hydrophilicity of the sample, leading to different hydration degrees in relation to the environment humidity.

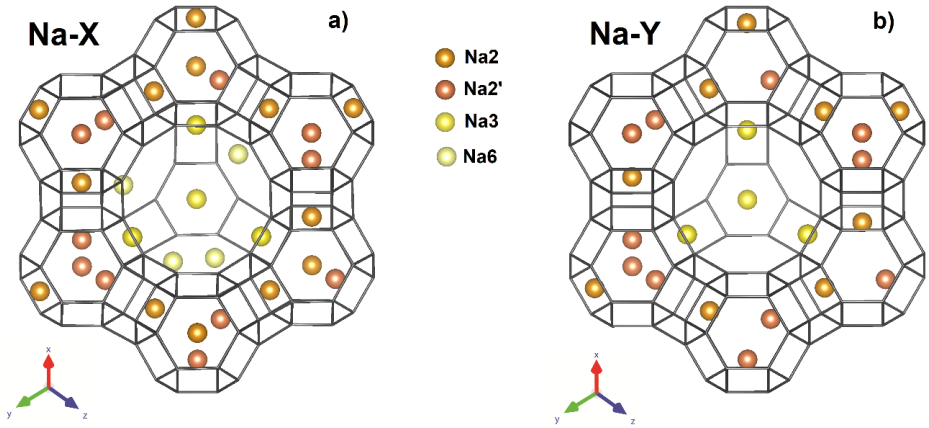

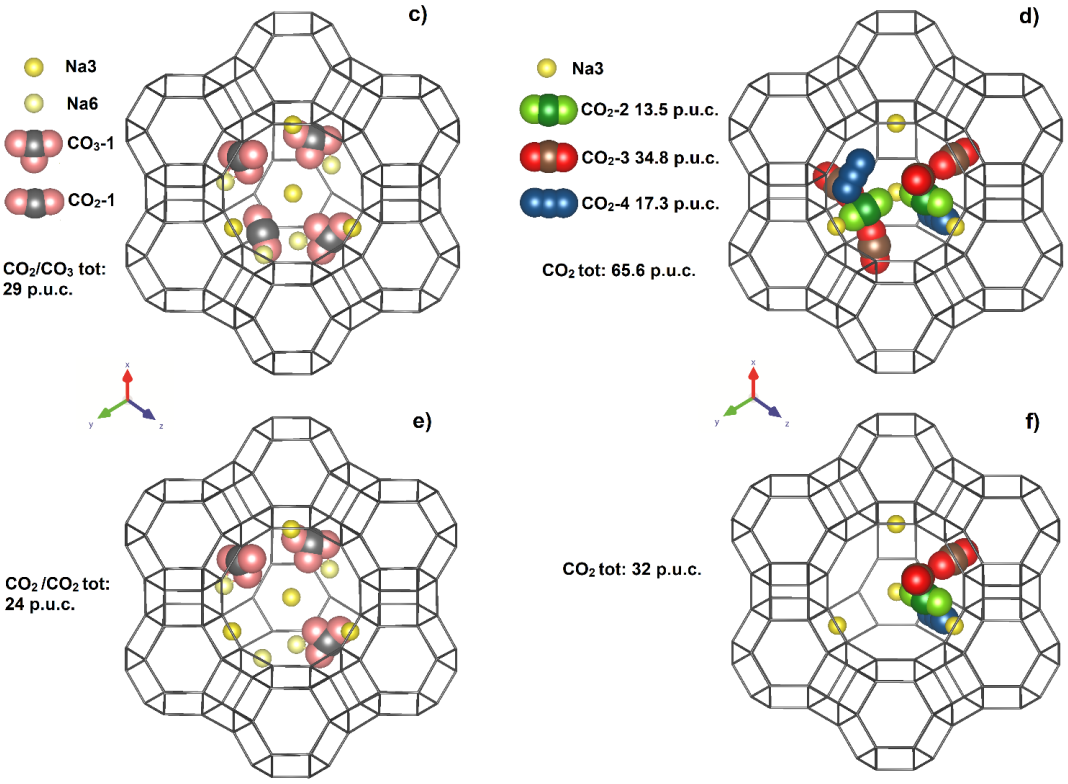

Figure 3. Structures of the zeolite samples under different conditions: (a) Na-X-*RT*, (b) Na-Y-*RT*, (c) Na-X-*CO*$_2$ (after CO_2 adsorption), (d) Na-Y-*CO*$_2$ (after CO_2 adsorption), (e) Na-X-*AP* (after CO_2 desorption), and (f) Na-Y-*AP* (after CO_2 desorption); a, b: the Na sites are drawn according to their occupancy factors; c, d, e, f: only the Na sites in the supercage are shown. Water molecules are not shown for sake of clarity.

Structural features of dehydrated nanosized FAU zeolites

The removal of water is a fundamental step for the use of FAU zeolites as adsorbents, since most of the porosity is occupied by H_2O molecules, thus hindering the penetration of other species under ambient condition. The HT treatment at 250°C seems to be not completely effective in dehydrating the Na-X sample since the structural refinement shows the presence of about 38 residual H_2O molecules. On the contrary, sample Na-Y was successfully dehydrated under the HT treatment at 250°C. Once the samples were brought back to *RT* conditions, due to their strong hydrophilic character, several H_2O molecules (probably migrating from the powder that was not

heated by the gas blower)- were re-adsorbed and 126 and 35 H_2O molecules p.u.c. were located in samples Na-X-*D-RT* and Na-Y-*D-RT*, respectively, (Table S2 and Scheme 1).

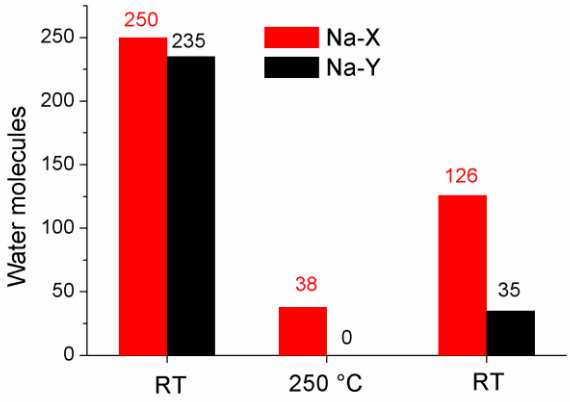

Scheme 1. Number of H_2O molecules in as-prepared Na-X and Na-Y zeolites at room temperature (Na-X -*RT*, Na-Y-*RT*), at 250° C and under vacuum ($5\cdot 10^{-3}$ Torr) (Na-X-*D-HT*, Na-Y-*D-HT*) and back to *RT* (Na-X-*D-RT*, Na-Y-*D-RT*) as determined by *in situ* XRPD and Rietveld refinement.

Structural features of nanosized FAU zeolites after adsorption of CO_2

The adsorption of CO_2 by the Na-X and Na-Y samples was followed by *in situ* XRPD. The host-guest and guest- guest interactions are discussed in this section. The intrinsic limit of the X-ray diffraction analysis, i.e., the determination of an average structure for the material under study, has to be taken into account

In the supercage of the Na-X sample the presence of four peak in the Differences Fourier Maps characterized by distances between 1.25 and 1.35 Å (C11-O11=1.30; C11-O12=1.25; C11-O13=1.34 see table S3) and by the geometry reported in Figure 4, suggested the authors the presence of a bi-dentate bicarbonate groups (labelled CO_3-1, Figure 3c, Tables S2 and S3). This was probably formed as a consequence of the interaction between the adsorbed CO_2 and the residual H_2O molecules. The sodium cations hosted in the supercage (Na6 site) are not shielded by the framework and thus can be responsible for the CO_2 polarization. The preferential formation of bicarbonate groups, associated to the presence of cations in this site (site III according to Ref.[24~~21~~]), has been already discussed in Ref. [25]. The position of ~~O~~one of the oxygens forming the CO_3 group (site O13, Table S2) corresponds to that of the H_2O molecule W8 in the dehydrated phase at room temperature (Na-X-*D-RT*). The presence of water during the CO_2 adsorption has been demonstrated

to favor the formation of bicarbonates species via hydroxyl group formation[26]. From the inspection of Figures 3c and 4, one can argue that the geometry of group CO_3-1, does not perfectly fit that of a bicarbonate group (i.e. with the angle O-C-O = 120°). This could be an artefact derived from the average structure determined by X-ray diffraction and can be attributed to the presence, in the same crystallographic positions, of a second configuration consisting of a CO_2 linear molecule and a water molecule, alternatively present (Figure 4).

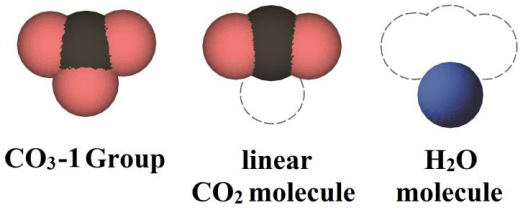

Figure 4. Possible configurations of the CO_3-1 group in Na-X-*CO_2* sample.

Assuming the alternative existence of CO_3, CO_2 and H_2O it is impossible to establish the relative amount of the three species. However, assuming the only presence of the bicarbonate, the total number of bicarbonate groups would be 29 (i.e. 3.6 molecules in each supercage). The distribution of the bi-dentate bicarbonate groups, bonded to Na cations, present in one supercage is shown in Figure 5.

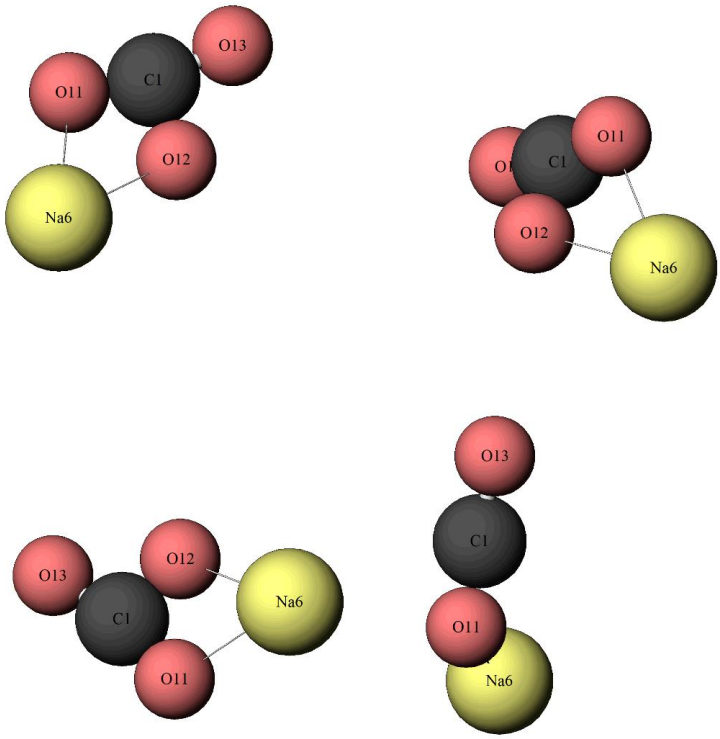

Figure 5. Possible distribution of CO_3 groups and Na6 cations in the supercage of the Na-X-*CO_2* sample, taking into account their occupancy factors and distances (only bonded Na6 are drawn).

During the CO_2 adsorption, additional 35 H_2O molecules are delivered to the Na-X zeolite sample accounting for a total of 138 re-adsorbed H_2O molecules; the additional water probably came from the CO_2 bottle or from the gas lines.

In the Na-Y zeolite only CO_2 molecules are hosted in the supercage, accounting for a total amount of 66 molecules. All the physisorbed CO_2 occupy three different positions as shown in Figures 3d and 6: (1) CO_2-2 (see Tables S2 and S3 for structural details), accounting for 14 molecules p.u.c. (i.e. 1.8 molecules in each supercage, in green in Figures 3d and 6); (2) CO_2-3: lying in the 12-ring windows between two supercages, accounting for 34 molecules p.u.c. (i.e. 4.3 molecules per supercage, in red in Figures 3d and 6); (3) CO_2-4, accounting for 18 molecules p.u.c. (i.e. 2.2 molecules per supercage, in blue in Figures 3d and 6). Even in the Na-Y zeolite further water molecules are adsorbed during the delivery of the CO_2 and as a whole 55 water molecules were found (not shown in Figure 3). Figure 6 shows a possible distribution of the CO_2 molecules, Na cations and W3 in the supercage taking into account their occupancy factors, distances and steric hindrance. Two crystallographic equivalent CO_2 clusters are located -formed by one CO_2-2, two

CO_2-3 and one CO_2-4 molecules- coordinated to Na3 cations and W3 via CO_2-2 and CO_2-4 molecules. Each cluster is in weak interaction with that hosted in the neighboring supercage via the CO_2-3 molecule sited in the 12 membered ring (Figure 7). The presence of these large clusters probably hinders further CO_2 adsorption.

The Na3 – CO_2 distances found for CO_2-2 and CO_2-4 are consistent with the linearly coordinated molecules as reported in Ref. [10]. On the contrary, CO_2–3 is not coordinating cations, but shows weak interactions with framework hydroxyl groups, as confirmed by the in situ FTIR results, where a band at 3742 cm^{-1}, characteristic of silanol groups, is present in the activated zeolite (SI, Figure S2). Despite the presence of H_2O molecules and cations coordinating CO_2 molecules, the presence of carbonates is not detected. This probably because Na3, contrariwise to what observed for Na6 in Na-X, is well compensated by framework oxygen atoms and thus is less effective in the CO_2 polarization.

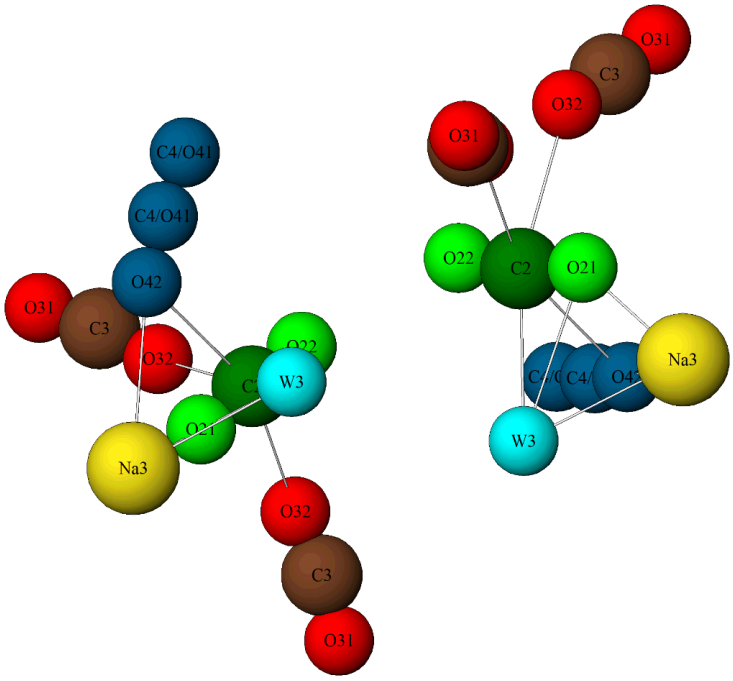

Figure 6. Possible distribution of CO_2 molecules, Na cations and W3 molecules in the supercage of the Na-Y-*CO_2* sample (only Na3 and W3 bonded to the clusters are drawn). The labels C2, O21 and O22 represent the CO_2-2 molecule, C3, O31 and O32 the CO_2-3 molecule and C4, O41 and O42 the CO_2-4 one.

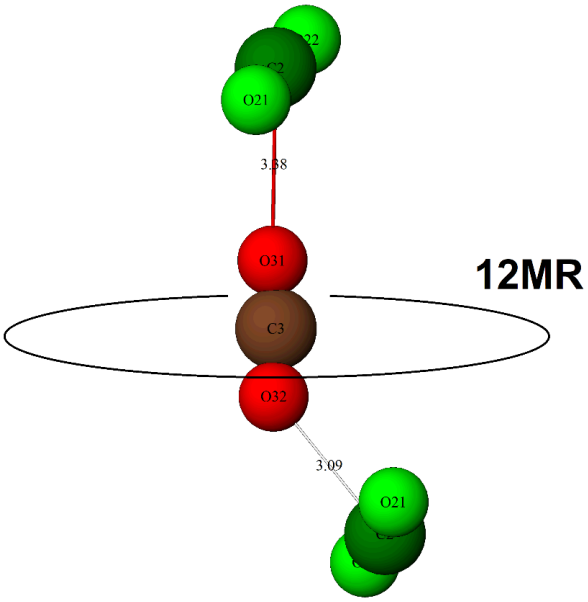

Figure 7. Interactions among CO_2-2 and CO_2-3 molecules in neighboring supercages in Na-Y-*CO_2* sample.

Structural features of nanosized FAU zeolites after desorption of CO_2

The persistence of CO_2 in the zeolite samples is strongly dependent on the host-guest interactions occurring during the absorption. In our experiments the desorption mechanism of CO_2 was studied under vacuum. The Na-X-*CO_2* sample is stable even under vacuum (5 x 10^{-3} Torr): from 29 CO_3 bi-dentate bicarbonate groups "nominally" adsorbed (see discussion above), about 24 remain in the pores even after pumping. On the contrary, in the Na-Y-*CO_2* sample, the pumping seems to be more effective than in the Na-X-*CO_2*. The CO_2 content decreases more than a half, i.e., about 31 CO_2 molecules p.u.c. from the original 66 still remain in the zeolite porosities. This is consistent with the fact that in the Na-Y-*CO_2* sample only physisorbed CO_2 molecules are present.

3.3 In situ FTIR characterization of nanosized FAU zeolites

In order to obtain more information about the adsorption mechanism of CO_2 in both Na-X and Na-Y zeolites, the CO_2 adsorption (at *RT*) and desorption (at *RT* and 250 °C) were monitored by *in situ* FTIR spectroscopy (Figures 8 and 9). In both cases, the absence of the band at 1627 cm^{-1} in the IR spectra of the activated samples counts for the successful removal of water. Nevertheless,

considering the results from the TG for sample Na-X (Figure 2), we may expect the presence of some residual water in the channels of zeolite at the activation temperature used (250° C).

Upon exposing Na-X to excess of CO_2, new sets of bands appear which were not present in the IR profile of the activated sample (Figure 8, Table 2). The new band at 2352 cm^{-1} corresponds to CO_2 physically adsorbed on the zeolite, the broadening of the feature is explained by the presence of excess CO_2 in the gas phase (non-adsorbed form). As a consequence of the high CO_2 content, the ^{13}C isotope (natural abundance) in CO_2 is detected at 2285 cm^{-1}. On the other hand, bands arising between 1707 and 1366 cm^{-1} are attributed to the chemisorbed CO_2. These correspond to different types of carbonates due to the participation of framework oxygen atoms (Table 2 and Figure 8). These results are consistent with the report by Busca[27] where bands are attributed to perturbed CO_2, bicarbonates, mono- and bi-dentate carbonates. Upon subjecting the samples to high vacuum desorption (~$5 \cdot 10^{-9}$ Bar) at room temperature, the band corresponding to physisorbed CO_2 (and CO_2 in gas phase) diminished drastically, while those corresponding to the chemisorbed CO_2 remained unchanged with the exception of the bands at 1484 and 1435 cm^{-1} (monodentate carbonates species) that slight increase. Such feature can result from the reaction of physisorbed CO_2 during evacuation. A quasi total desorption for the CO_2 at 250 °C was achieved; the spectrum highly resembles that of the activated sample.

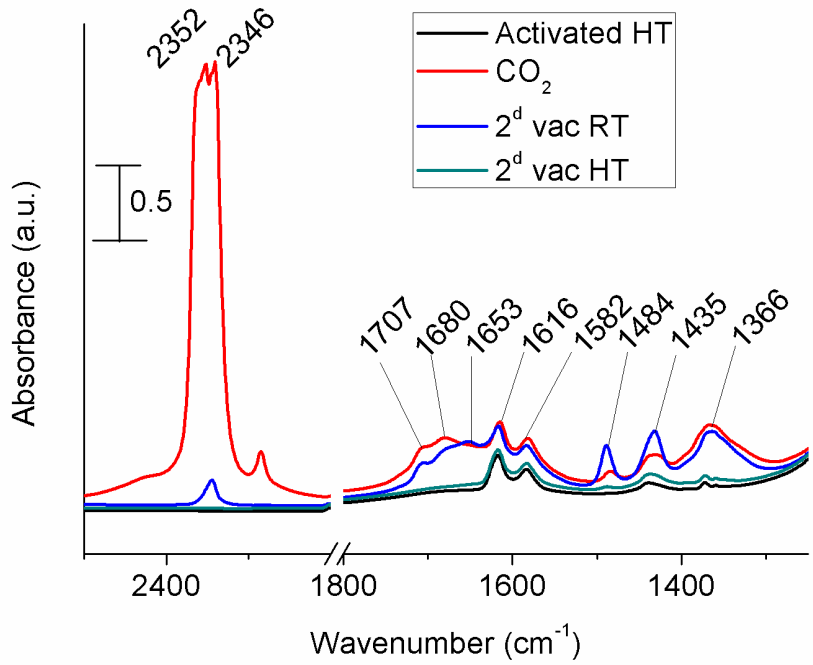

Figure 8. FTIR spectra of nanosized Na-X zeolite activated at 250 °C (black), after adsorption of 0.01 Bar CO_2 (red), under secondary vacuum (~$5 \cdot 10^{-9}$ Bar) at room temperature (blue), and under secondary vacuum (~$5 \cdot 10^{-9}$ Bar) and at 250 °C (green).

Table 2. FTIR bands and the corresponding assignments recorded for the Na-X nanosized zeolite under adsorption of 0.01 Bar CO_2.

Bands (cm^{-1})	**Assignements**	**FTIR band area (a.u.)**			
		Activated	**CO_2**	**2^d vac RT**	**2^d vac HT**
2352	Physisorbed CO_2	0	122.5	3.48	0
1707	CO_2 molecules Perturbed	0	5.15	3.16	0
1680 & 1366	Bicarbonates	0	27.83	25.10	1.13
1653	Residual acidity	0	7.35	9.98	0.49
1616	Water	0	3.28	3.10	0.16
1582	Bidentate carbonates	0	3.51	3.24	0.50
1484 & 1435	Monodentate carbonates	0	4.12	11.31	1.15

The adsorption of CO_2 on the Na-Y zeolite induced the formation of a band at 2354 cm^{-1} corresponding to the physisorbed CO_2 together with a set of bands related to chemisorbed CO_2 observed between 1750 and 1300 cm^{-1} (Figure 9, Table 3). Unexpectedly, signals of bicarbonates were detected at 1681 and 1364 cm^{-1} despite the activation at 250 °C which is enough to eliminate the water from the sample as evidence by TGA. One possible explanation for their existence is the reaction of incoming CO_2 with residual water (not deteced by IR) available in the zeolite channels or with the residual acid sites detected at 1653cm^{-1}.

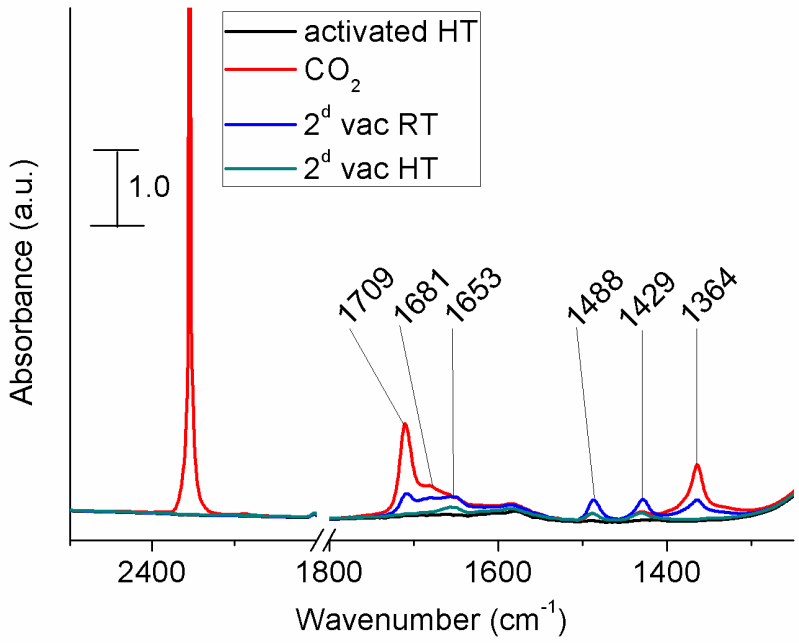

Figure 9. FTIR spectra of nanosized Na-Y zeolite under activation at 250 °C (black), after adsorption of 0.01 Bar CO_2 (red), under secondary vacuum (~$5 \cdot 10^{-9}$ Bar) at room temperature (blue), and under secondary vacuum (~$5 \cdot 10^{-9}$ Bar) and activation at 250 °C (green).

A desorption behavior similar to Na-X was recorded for Na-Y at *RT*: the band corresponding to physisorbed CO_2 disappeared completely, chemisorbed CO_2 (perturbed CO_2 and bicarbonates) decreased significantly, while the bands corresponding to monodentate carbonates and residual acidity increased. As shown in Figure 9 (green curve), an increase of the temperature up to 250 °C was required to almost fully desorb the chemisorbed CO_2. The latest spectrum (green) is very similar to that collected from the activated Na-Y (black), demonstrating the reversibility of CO_2 sorption within the Na-Y nanosized zeolite with minor residual acidity maintained.

,

Table 3. FTIR bands and the corresponding assignments recorded for the Na-Y nanosized zeolite under adsorption of 0.01 Bar of CO_2.

Bands (cm^{-1})	**Assignements**	**FTIR band area (a.u.)**

		Activated	CO_2	2^d vac RT	2^d vac HT
2354	Physisorbed CO_2	0	34.86	0.15	0
1709	CO_2 molecules perturbed	0	16.97	4.69	0.22
1681 & 1364	Bicarbonates	0	16.92	8.43	0.53
1653	Residual acidity	0	3.48	5.35	1.69
1488 & 1429	Monodentate carbonates	0	1.94	6.33	0.83

An interesting observation lies on the existence of bidentate carbonate in Na-X, but not in Na-Y. The lower Si/Al ratio of the Na-X sample induces a closer proximity of Al within the framework and then of Na cations, and thus higher possibilities for the formation of bidentate species exist.

4. Discussion

Nanosized Na-Y and Na-X zeolites show a different behavior in adsorbing/desorbing of CO_2. The main differences are related to the amount of CO_2 adsorbed and to their interaction with the zeolite framework and extra-framework species.

In this work, for the first time, the coupling of two complementary techniques (XRPD and IR) offers the opportunity to probe the CO_2 adsorption/desorption mechanisms at different levels (i.e. average structure by XRPD *vs* local structure by IR). In fact, the results for Na-Y XRPD are consistent with the presence of physisorbed CO_2 molecules only, while IR results show even the presence of mono dentate carbonates formed after framework oxygen interaction and bicarbonates probably formed due to the interactions with residual H_2O that unintentionally reentered the zeolite channel or residual acidic sites. The chemisorbed CO_2 species are probably present in very low amount that cannot be detected by X-ray diffraction. Regarding the nanosized Na-X zeolite, both physisorbed and chemisorbed species were detected by both the XRPD and IR techniques. In particular, XRPD indicates the presence of bicarbonate only, while IR detected even mono and bidentate carbonates.

The interpretation of the results relative to desorption deserves particular attention. From the spectroscopic investigations, it appears that, while the physisorbed species are removed from the zeolites channel by pumping under secondary vacuum ($\sim 5 \cdot 10^{-9}$ Bar) at room temperature, carbonates and bicarbonates remain in the pores. While the carbonates are completely removed from the pores under heating at 250 °C. On the contrary from the XRPD results it appears that both chemisorbed and physisorbed species are only partially removed from the porosity. This is due to

different vacuum conditions of the two devices (~$5 \cdot 10^{-9}$ Bar for IR experiment *vs* ~$6 \cdot 10^{-7}$ Bar for XRPD one).

Previous studies performed on this topic shed light on different factors that may influence the CO_2 adsorption in zeolites, finding that in addition to the structural and chemical features of the zeolite samples, other aspects must be considered[26~~23~~]. In fact, the carbonates/bicarbonates formation plays a key role during the carbon dioxide adsorption, the presence of these species might decrease the accessibility of CO_2 molecules limiting the adsorption and hindering the regeneration capacity in successive adsorption-desorption cycles[26~~23~~-28]. The formation of carbonates, in most of the cases, is associated with the presence of cations in the electrostatically less-shielded type III site, located in the FAU supercage, present only in the Na-X zeolite[25~~22~~]. In our study the presence of carbonates/bicarbonates was evidenced in both Na-X and Na-Y samples, even if in very different amount.

The influence of water in the adsorption of CO_2 is of paramount importance, being water one of the key components in flue gas. The presence of H_2O molecules in the zeolite cavities during the CO_2 adsorption seems to favor the formation of bicarbonates species via hydroxyl group reaction[4,26~~23~~]. Different behaviors in relation to H_2O content were reported. Brandani and co-workers[29] observed that even small amount of water can inhibit the CO_2 adsorption on different cationic forms of zeolite X. Bertsch and co-workers[30] suggest that the presence of small amount of pre-adsorbed water greatly accelerate the rate of carbon CO_2 adsorption, presumably by catalyzing the chemisorption step.

In our study the presence of H_2O molecules favors the formation of bicarbonates in nanosized Na-X zeolite. The small amount of bicarbonate found in the Na-Y should be due to the use of moist CO_2.

Two recent papers investigated from the structural point of view the CO_2 adsorption in micron-sized zeolite Y by neutron powder diffraction[12~~12~~] and Synchrotron X-ray Powder diffraction[13~~13~~]. In both papers only physisorbed CO_2 was found, which is in agreement with our work for the nanosized Na-Y. The discrepancies on the number of molecules measured is due to different pressure conditions used for the CO_2 adsorption and to the different crystal size of the samples studied. In fact ~~in~~ the crystal ~~nano~~size~~d~~ of the zeolites analyzed in this work favored the adsorption, leading to an higher CO_2 adsorption capacity.

Wong et al.[12] found two crystallographically independent CO_2 sites, bonding the Na cations, in the supercage. Arletti and co-workers[13] found the evidence of tetrameric clusters of CO_2 molecules connected by water bridges to the Na cations of adjacent FAU supercages. These clusters, even if placed in the same portion of the supercage, are different from that found in this

Formattato: Apice

Formattato: Apice

Formattato: Apice

Formattato: Apice

work, consisting of three/five CO_2 molecules. This could be dictated by the higher amount of molecules adsorbed in consequence of the higher CO_2 pressure applied in the present work. In both papers, a CO_2 molecule located in the supercage (O16-C15-O16[12] and CO_2b[13]) corresponds to the CO_2-4 molecule of this work. In addition, the position of CO_2-3 molecule of this work, in the window between two supercages, almost corresponds to that reported in Ref. [12] (O12-C11-O13), but shifted of about 1.9 Å along the molecule axis.

5. Conclusions

The adsorption of CO_2 in two FAU zeolite samples with nanosized dimensions, one corresponding to zeolite Na-X (Si/Al=1.24) and the other to Na-Y (Si/Al=2.54) was studied by X-ray powder diffraction and FTIR spectroscopy. In the case of nanosized Na-X, 29 CO_2 molecules p.u.c., while in the nanosized Na-Y 66 molecules p.u.c. were adsorbed. The structural refinement results are in line with the FTIR spectroscopy analysis, representing the presence of physisorbed CO_2 in both zeolites, while the chemisorbed CO_2 was not detected in the Na-Y by XRPD probably due to the low amount. In the case of Na-X, on the contrary, the presence of the Na6 cations in the supercage and of water molecules induces the formation of bidentate bicarbonate groups, identified by both XRPD and FTIR.

The release of adsorbed species under high vacuum treatment ($5 \cdot 10^{-9}$ Bar) from the nanosized Na-Y zeolite, where the CO_2 is mainly physisorbed, is almost complete. On the contrary, for the nanosized Na-X the vacuum treatment induces the desorption of physisorbed CO_2 only, while the chemisorbed species remain trapped in the pores. Only high temperature treatment (above 300 °C) effectively removes the carbonates.

The FAU zeolite with nanosized crystals are considered to be used for target CO_2 delivery in biomedicine where the ratio of physisorbed and chemisorbed CO_2 is of great importance.

Acknowledgment

Authors thank Dr. Carlotta Giacobbe and all the staff of ID22 beamline at ESRF (Grenoble, France), for their help during XRPD data collections. Se lo mettiamo nella relazione Zapping bisogna e I ringraziamenti

Supplementary Material deposited:

Table S1. Lattice parameters and Rietveld refinement according factors for Na-X and Na-Y structures under the different conditions.

Table S2. Atomic coordinates, occupancy factors and thermal parameters for Na-X (a) and Na-Y (b) structures under the different conditions.

Table S3. Selected framework and extraframework distances for Na-X (a) and Na-Y (b) structures under the different conditions.

Figure S1 Observed (red dash marks) and calculated (green line) diffraction patterns and final difference curve (purple line) from Rietveld refinements for Na-X-RT (a); Na-Y-RT(b); Na-X-D-RT (c); Na-Y-D-RT (d); Na-X-CO2 (e), Na-Y-CO2 (f); Na-X-AP (g); Na-Y-AP (h).

Figure S2. FTIR spectra of activated zeolite samples (250 °C) revealing the band at 3742 cm^{-1} characteristic of silanol groups.

Formattato: Tipo di carattere: 12 pt

Formattato: Tipo di carattere: 12 pt

Formattato: Tipo di carattere: 12 pt

Table of Contents

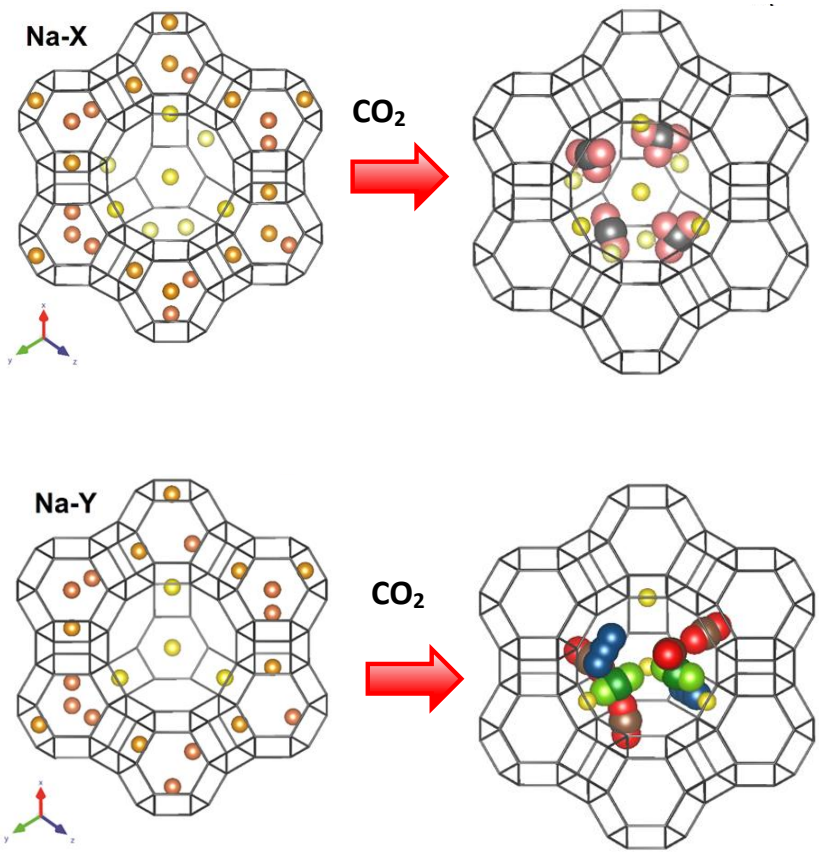

Nano Na-X and Na-Y before and after CO_2 adsorption

References

(1) Yang, H.; Xu, Z.; Fan, M.; Gupta, R.; Slimane, R.B.; Bland, A.E.; Wright, I. Progress in carbon dioxide separation and capture: a review. *J. Environ. Sci.* **2008**, 20, 14-26.
(2) Morris, R.E.; Wheatley, P.S. Gas storage in nanoporous materials. *Angew. Chem.* **2008**, 47, 4966-4981.
(3) Choi, S.; Drese, J.H.; Jones, C.W. Adsorbent materials for carbon dioxide capture from large anthropogenic point sources. *Chem. Sus. Chem.* **2009**, 2, 796-854.
(4) Siriwardane, R.V.; Shen, M.S.; Fisher, E.P.; Poston, J.A. Adsorption of CO_2 on Molecular Sieves and Activated Carbon. *Energy Fuels*. **2001**, 15, 279-284.
(5) Zukal, A.; Mayerová, J.; Kubu, M. Adsorption of carbon dioxide on high-silica zeolites with different framework topology. *Top Catal.* **2010**, 53, 1361-1366.
(6) Baerlocher, C.; McCusker, L.B. Olson, D.H. *Atlas of Zeolite Framework Types sixth ed.* Elsevier, Amsterdam, **2007**.
(7) Lee, J.S.; Kim, J.H.; Kim, J.T.; Suh, J.K.; Lee J.M.; Lee, C.H. Adsorption equilibria of CO_2 on zeolite 13X and zeolite X/activated carbon composite. *J. Chem. Eng. Data*. **2002**, 47, 1237-1242.
(8) Lu, C.; Bai, H.; Wu, B.; Su, F.; Hwang, J.F. Comparative study of CO_2 capture by carbon nanotubes, activated carbons, and zeolites. *Energy Fuels.* **2008**, 22, 3050-3056.
(9) Siriwardane, R.V.; Shen, M.S.; Fisher, E.P. Adsorption of CO_2 on zeolites at moderate temperatures. *Energy Fuels.* **2005**, 19, 1153-1159.
(10) Maurin, G.; Llewellyn, P.L.; Bell, R.G. Adsorption mechanism of carbon dioxide in faujasites: grand canonical Monte Carlo Simulations and microcalorimetry measurements. *J. Phys. Chem.* **2005**, 109, 16084-16091.
(11) Plant, D.F.; Maurin, G.; Jobic, H.; Llewellyn, P.L. Molecular dynamics simulation of the cation motion upon adsorption of CO_2 in faujasite zeolite systems. *J. Phys. Chem.* **2006**, 110, 14372-14378.
(12) Wong-Ng, W.; Kaduk, J.A.; Huang, Q.; Espinal, L.; Li, L.; Burress, J.W. Investigation of NaY Zeolite with adsorbed CO_2 by neutron powder diffraction. *Microporous Mesoporous Mater.* **2013**, 172, 95-104.
(13) Arletti, R.; Gigli, L.; Di Renzo, F.; Quartieri, S. Evidence for the formation of stable CO_2 hydrates in zeolite Na - Y: Structural characterization by synchrotron X- ray powder diffraction. *Microporous Mesoporous Mater.* **2016**, 228, 248-255.
(14) Mintova, S.; Jaber, M.; Valtchev, V. Nanosized microporous crystals: emerging applications. *Chem. Soc. Rev.* **2015**, 44, 7207-7233.
(15) Komaty, S.; Anfray, C.; Zaarour, M.; Awala, H.; Ruaux, V.; Valable, S.; Mintova, S. A Facile Route toward the Increase of Oxygen Content in Nanosized Zeolite by Insertion of Cerium and Fluorinated Compounds. *Molecules*. **2018,** 23, 37- 40.
(16) Clément, A. ; Biao, D.; Komaty, S.; Mintova, S.; Valable, S. Acute toxicity of silver free and encapsulated in nanosized zeolite for eukaryotic cells. *Appl. Mater. & Interf.*, **2017**, 9, 13849–13854.
(17) Georgieva, V.; Retoux, R.; Ruaux, V.; Valtchev,V.; Mintova, S. Detection of CO_2 and O_2 by iron loaded LTL zeolite films. *Frontiers of Chem. Sci. and Engin.* **2018**, 12, 1294–102.
(18) Awala, H.; Gilson, J.-P.; Retoux, R.; Boullay, P.; Goupil, J.-M.; Valtchev, V.; Mintova, S. Template-free nanosized faujasite-type zeolites. *Nat. Mater.* **2015**, 14, 447–451.
(19) Larson, A.C.; Von Dreele, R.B. *General Structure Analysis System "GSAS"*, Los Alamos National Laboratory Report LAUR, **1994**, 86-748.
(20) Toby, B.H. A graphical user interface for GSAS. *J. Appl. Crystallogr.* **2001**, 34, 210-213.

Formattato: Pedice

Formattato: Pedice

Formattato: Pedice

Formattato: Pedice

(21) Su, H.; Kim, H.S.; Seo, S.M.; Ko, S.O.; Suh, J.M.; Kim, J.H.; Lim, W.T. Location of Na+ Ions in Fully Dehydrated Na+-saturated Zeolite Y (FAU, Si/Al = 1.56). *Bull. Korean Chem. Soc.* **2012**, 33, 8, 2785-2788.
(22) Olson, D.H. Reinvestigation of the crystal structure of the zeolite hydrated NaX. *J. Phys. Chem.* **1970**, 74, 2758-2764.
(23) Thomson, P.; Cox, D.E., Hastings J.B. Rietveld refinement of Debye-Scherrer synchrotron X-Ray data from Al_2O_3. *J. Appl. Crystallogr.* **1987**, 20, 79-83.
(24) Frising, T., Leflaive P. Extraframework cation distributions in X and Y faujasite zeolites: A review. *Microporous Mesoporous Mater.* **2008**, 114, 27-63.
(25) Jacobs, P.A.; Van Cauwelaert, F.H.; Vansant, E.F.; Uytterhoeven, J.B. Surface probing of synthetic faujasites by adsorption of carbon dioxide. Part 1.—Infra-red study of carbon dioxide adsorbed on Na-Ca-Y and Na-Mg-Y zeolites. *J. Chem. Soc.* **1973**, 1056-1068.
(26) Bonenfant, D.; Kharoune, M.; Niquette, P.; Mimeault, M.; Hausler, R. Advances in principal factors influencing carbon dioxide adsorption on zeolites. *Sci. Technol. Adv. Mater.* **2008**, 9, 013007.
(27) Busca, G. Acidity and basicity of zeolites: A fundamental approach. *Microorous . Mesoporous Mater.* **2017**, 254, 3-16.
(28) Angell, C.L.; Howell, M.V. Infrared spectroscopic investigations of zeolites and adsorbed molecules. Part V. Carbon dioxide. *Can. J. Chem.*, **1969**, 47, 3831-3836.
(29) Brandani. F.; Ruthven, D.M. The Effect of Water on the Adsorption of CO_2 and C_3H_8 on Type X Zeolites. *Ind. Eng. Chem. Res.*, **2004**, 43, 8339-8344.
(30) Bertsch, L.; Habgood, H.W. An Infrared Specroscopic study of the adsorption of water and carbon dioxide by Linde molecular sieve X1. *J. Phys. Chem.*, **1963**, 67, 1621-1628.

Formattato: Pedice
Formattato: Pedice
Formattato: Pedice